RSC Advances

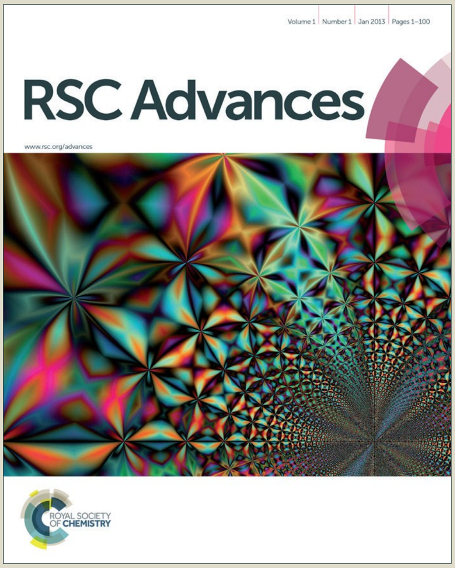

ROYAL SOCIETY
OF CHEMISTRY

www.rsc.org/advances

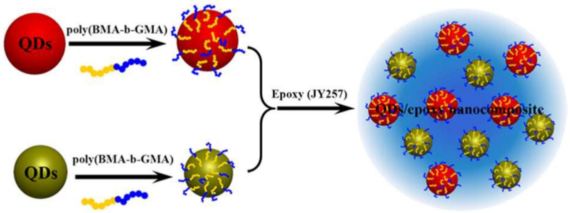

The QDs/epoxy nanocomposite expressed highly transparency and luminescence through introducing poly(BMA-b-GMA) block copolymer as compatibilizer at the interface between QDs and epoxy matrix.

Synthesis of poly(n-butyl methacrylate)-(glycidyl methacrylate) block copolymer and its compatibilization at the interface of QDs/epoxy nanocomposite for white LED encapsulation

Lanlan Chen[a], Chen Zhang[a], Zhongjie Du[a], Hangquan Li[a], Li Zhang[b], Wei Zou[a]*

[a]Key Laboratory of Carbon Fiber and Functional Polymers (Beijing University of Chemical Technology, Ministry of Education), Beijing 100029, PR China

[b]China National Chemical Corporation, Beijing 100080, PR China

Abstract

A facile approach for synthesizing transparent luminescent quantum dots (QDs)/epoxy nanocomposite had been presented by introducing poly(n-butyl methacrylate)-(glycidyl methacrylate) block copolymer as compatibilizer at the interface between QDs and epoxy matrix. Poly(n-butyl methacrylate)-(glycidyl methacrylate) block copolymer denoted as poly(BMA-b-GMA) was successfully synthesized by atom transfer radical polymerization. Then it was designed to solve the problem of polar mismatch at nanocomposite interface because that butyl could assemble with oleic acid ligand on QDs and glycidyl could match epoxy matrix respectively. Thus the formed compatible interface of QDs/epoxy nanocomposite directly avoided aggregation of QDs, and eventually increased transparency and luminescence of nanocomposite. The as-prepared highly transparent and luminescent QDs/epoxy nanocomposite had potential in white LED encapsulation.

Keywords: Quantum dot; Block copolymer; Interface; Nanocomposite; Optical properties

Correspondence to: Wei Zou (E-mail: zouwei@mail.buct.edu.cn; Tel./fax :+86 10-64430908)

1. Introduction

Semiconductor quantum dots (QDs) have drawn enormous attention in the past decade due to their unique optical properties[1,2] and potential application to epoxy matrix nanocomposite as encapsulating material of light-emitting diode (LED).[3-5] For this application, good dispersion of QDs in epoxy matrix was a very important factor.[6,7] However, when QDs were added in organic epoxy matrix, there was strong tendency for them to aggregate due to the high surface area and poor compatibility between QDs and epoxy matrix.[8-10] This not only affected optical transparency of the resultant nanocomposite, but also limited luminescent properties and device performances.

In order to improve the dispersion of inorganic QDs within organic polymer matrices, surface modification of QDs was the most promising method.[11-13] After agent with similar polar or chemical structure to target matrix was grafted onto the surface of QDs, the formed compatible interface could enhance its dispersibility.[14,15] Klaus Mullen[16] synthesized ZnO QDs/PMMA nanocomposite using amphiphilic statistical copolymer as compatibilizer at the interface. With functional hydrophobic chains on the surface of ZnO QDs, blending of ZnO QDs in PMMA afforded transparent nanocomposite films avoiding particle aggregated. Su Chen[17] used 2-mercaptoethanol as the organic ligand to obtain hydroxyl-coated functional CdS nanocrystals, allowing them to react with toluene 2, 4-diisocyanate (TDI) reagent and then to fabricate well-defined transparent CdS nanocrystal-PU nanocomposite hybrids in situ. The obtained nanocomposite exhibited good optical properties. Min Zhi Rong[18] modified ZnO QDs by epoxy silane. Thereby, a highly transparent and luminescent ZnO QDs/epoxy nanocomposite was obtained. In our previous works, functionalized CdSe@R (R=COOH, NH_2 or epoxy) had been prepared.[19-21] CdSe@R covalently bonded with epoxy in curing period, thus non polar CdSe was homogenously dispersed in polar epoxy matrix because of enhanced compatibility. Consequently, transparency and luminescence of nanocomposites were improved at the same time.

In this work, poly(n-butyl methacrylate)-(glycidyl methacrylate) block copolymer denoted as poly(BMA-b-GMA) was successfuly synthesized to assemble onto the surface of QDs (Scheme 1). Firstly, atom transfer radical polymerization (ATRP) was utilized to synthesize molecular weight controlled copolymer compatibilizer. And then, the process of compatibilizer assembly behavior at the interface was described by kinetic and thermodynamics. Besides, the influences of compatibilizer on the QDs optical properties were investigated after assembly. Finally, crucial relationships between interface structure and properties of QDs/epoxy nanocomposite were clarified. Moreover, green and red emission CdS coated CdSe QDs mixture were dispersed in epoxy resin, and the resulted dual QDs/epoxy nanocomposite was used as encapsulating material of LED for obtaining warm white light.[22,23] A white LED with good performance was fabricated by coating the dual QDs/epoxy nanocomposite onto a blue light emitting (465nm) InGaN chip.

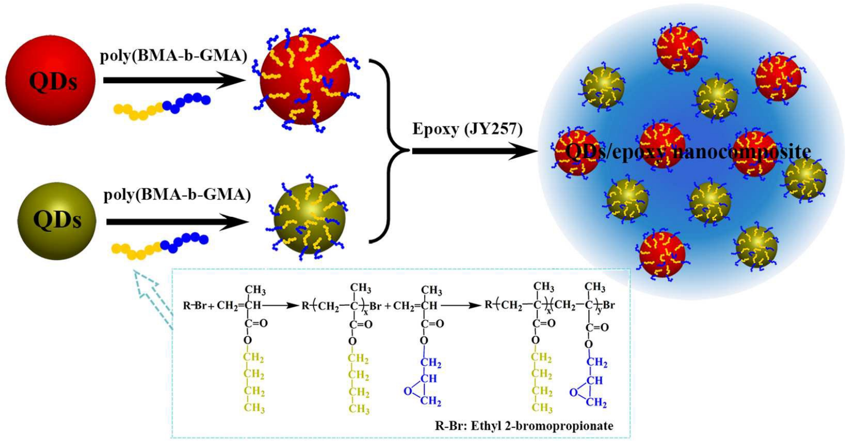

Scheme 1. Schematic presentation of QDs functionalization and QDs/epoxy

nanocomposite fabrication

2. Experimental Part

2.1 Materials

Ethyl 2-bromopropionate (EPN-Br), CuBr, toluene, n-butyl methacrylate (BMA), N,N,N',N',N"-pentamethyldiethylenetriamine (PMDETA), HCl, glycidyl methacrylate (GMA), selenium, sulfur, cadmium oxide, acetone, tetrahydrofuran, oleic acid and triethylenetetramine were purchased from Vas Chemicals Co., China. 1-Octadecene (90%) and tri-n-octylphosphine (90%) were purchased from Alfa Aesar, USA. Epoxy (JY257) (Epoxy value is 0.53-0.55 mol/100g; Viscosity is 500-1000 mPa.s; Specific gravity is 1.14-1.16 g/cm^3) was purchased from Changshu jaffa chemical co., LTD.

2.2 Preparation of poly(BMA-b-GMA) copolymer compatibilizer by ATRP

Polymerization was carried out using CuBr as a catalyst, PMDETA as a ligand and EPN-Br as a initiator under nitrogen atmosphere. A stock solution containing the toluene (3.15 mL), BMA (3.15 mL) and PMDETA (0.21 mL) along with CuBr (0.143 g) was prepared and sealed with rubber septum. The solution was degassed by three vacuum-nitrogen cycles and stirred at room temperature. The initiator EPN-Br (0.14 mL) was then added to solution with a syringe and the solution was again purged with nitrogen. Finally the flask containing solution was kept in oil bath and maintained at 50 ^{o}C with magnetic stirring for 90 min. Then the flask was removed from the oil bath and the mixture was diluted with 50 mL THF. The solution was passed over a column with neutral alumina to remove the catalyst. Then the rest of the solution was concentrated by rotary evaporation, and the product (PBMA-Br) was dried at 60 ^{o}C under vacuum.

The copolymerization was carried out using PBMA-Br as macroinitiator under the same concentration ratios $[GMA]_0$:$[CuBr]_0$:$[PMDETA]_0$:[PBMA-Br$]_0$=20:1:1:1. The reaction was proceeded under the same conditions for 90 min, and then the flask was removed from the oil bath and the mixture was diluted with 50 mL THF. The solution was passed through a basic alumina column to remove the catalyst. After concentration by rotary evaporation, the final product poly (BMA-b-GMA) was dried at 60 °C under vacuum for further use.

2.3 Preparation of CdS coated CdSe QDs functionalized with block copolymer

CdS coated CdSe QDs were prepared and purified according to the method previously used in our team. Through changing the capping time from 3 to 40 min, the CdS coated CdSe QDs with desired wavelength were obtained.[24] The QDs used in this study were green and red light emitting CdS coated CdSe QDs. The purified QDs were dispersed in 5 wt% poly (BMA-b-GMA)/THF solution under ultrasonic for 30 min. After self-assembly, the mixture was centrifuged at 6000 rpm for 10 min. The product was collected and dried at 30 ^{o}C under vacuum.

2.4 Preparation of QDs/epoxy nanocomposite

The functionalized QDs (60 mg) and epoxy (17.65 g) were mixed and then the curing agent triethylenetetramine (2.29 g) was added with stirring. The mixture was out-gassed in a vacuum oven at 30 ^{o}C for 20 min, then cast into a mould and cured in a vacuum oven at 40 ^{o}C for 2 h.

2.5 Measurements

The molecular weights (Mn) and molecular weight distributions (Mw/Mn) of the samples were measured using gel permeation chromatography (GPC; Waters GPC 515–2410). THF was filtered and used as the eluent at a flow rate of 1.0 mL/min. Samples for the analysis were prepared as 2 mg/mL solutions in THF and filtered through 0.45 μm filters prior to injection. UV–vis absorption and transmittance spectra were recorded using Hitachi U-3010 from 350 nm to 800 nm (Scan Speed:

300 nm/min). The excitation and emission spectra were recorded using F-4500 fluorescence spectrophotometers (slit width was 5 nm, and excited light of the emission spectrum was 465 nm). Enthalpies of dissolution were obtained using a Setaram C-80 Calvet twin microcalorimeter. Sizing of QDs particles were conducted by dynamic light scattering (DLS) using a Zetasizer Nano ZS (Malvern Instruments, Southborough, MA) with a laser of wavelength of 633 nm at a 173° scattering angle. The optical properties of the LED were measured by an MCPD-7000 photodetector.

The epoxy value was titrated by HCl-Acetone method. The HCl-Acetone solution was prepared based on the volume ratio of HCl-Acetone (2 mL HCl: 30 mL acetone), and stored in a glass bottle in case of need. About 0.5 g of the sample was dissolved in 20 mL of HCl-Acetone solution. After 30 min, 5 drops of phenolphthalein indicator were added, and the excess HCl was titrated by NaOH (0.10 mol L^{-1}). The epoxy value (EV, mol 100 g^{-1}) was calculated by the following formula:

$$EV = \frac{(V_0 - V)\times C}{W} \times 100$$

where C is the concentration of NaOH standard solution (mol L^{-1}), V_0 is the blank consumption of NaOH standard solution (L), V is the sample consumption of NaOH standard solution (L), and W is the weight of the sample (g).

Photoluminescence quantum yields (QY) were obtained by comparison with a standard (Rhodamine 6G in ethanol) and using data derived from the luminescence and the absorption spectra, as follows:

$$\phi_{QDs} = \phi_s \left(\frac{A_{QDs}/I_{QDs}}{A_s/I_s}\right)\left(\frac{n_1}{n_2}\right)^2$$

Where φ, A and I were the quantum yield, luminescent density and absorbant intensity, respectively. The subscript S was the standard material. n_1, n_2 was the reference index of THF and ethanol, respectively.

3. Results and discussion

3.1 ATRP of molecular weight controlled poly(BMA-b-GMA)

The effect of various components of ATRP (polymerization temperature, reaction time, concentration of reaction solution, molar ratio of monomer and initiator, and feed order of monomers) were examined to achieve controlled copolymerization conditions of each block molecular weight (Fig. S1-S5). Based on the above investigation, molecular weight controlled copolymers were synthesized as template for modification of QDs (PBMA segment molecular weight 420, 850, 1700 and PGMA segment molecular weight 850, respectively; PBMA segment molecular weight 850 and PGMA segment molecular weight 420, 850, 1700, 2130, respectively).

3.2 Study on the compatibilization mechanism

3.2.1 The influences of PBMA segment molecular weight on thermodynamics and dynamics of compatibilizers assembled on QDs surface

The experiments for adsorption thermodynamics of compatibilizers on quantum dots surface were carried out at varying temperatures (293, 303, 313 and 323 K). The thermodynamic calculation formulas were as follows:

$$K_c = \frac{C_{Ae}}{C_e} \tag{1}$$

$$\Delta G = -RT \ln K_c \tag{2}$$

$$\ln K_c = \frac{\Delta S}{R} - \frac{\Delta H}{RT} \tag{3}$$

where K_c was the ratio of adsorbate capacity on adsorbent at equilibrium (C_{Ae}) to the remaining adsorbate concentration in solution at equilibrium (C_e); T was absolute temperature in Kelvin; R (8.314 J/mol K) was the universal gas constant; ΔH and ΔS

were standard enthalpy and standard entropy; ΔG was standard free energy. The ΔH and ΔS were calculated from the slope and intercept of the linear plot of $\ln K_c$ versus 1/T (Fig. 1), the results were listed in Table 1.

As shown in Table 1, the ΔG value was negative, indicating the adsorption process of compatibilizers was spontaneous process. The negative value of ΔH indicated the adsorption process of compatibilizers was exothermic, and the compatibilizer with lager PBMA segment molecular weight more easily adsorbed to the surface of the QDs.

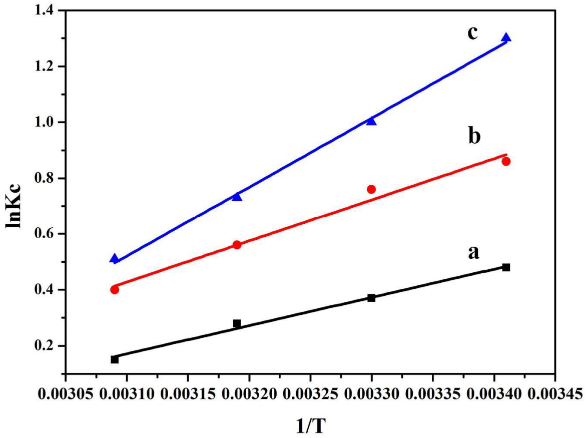

Fig. 1 Plot of $\ln K_c$ versus 1/T for estimation of thermodynamic parameters. (a, b, c were compatibilizers with PGMA segment molecular weight 850, and PBMA segment molecular weight 420, 850, 1700, respectively.)

Table 1 Thermodynamic parameters for adsorption of compatibilizers on quantum dots surface

Compatibilizers	T(K)	ΔG (KJ/mol)	ΔH (KJ/mol)
a	293	-1.17	-8.38
	303	-0.93	
	313	-0.73	
	323	-0.40	
b	293	-2.09	-12.25
	303	-1.91	
	313	-1.46	
	323	-1.07	
c	293	-3.17	-20.53
	303	-2.52	
	313	-1.90	
	323	-1.37	

Fig. 2 illustrated the effect of contact time on the adsorption process. The adsorption equilibrium could be achieved within 100 min. At this moment, the adsorption value of the compatibilizer with PBMA segment molecular weight 420 was 16.5 mg/g, and then the adsorption increased a little as the time increased. Moreover, it could be seen that the adsorption rate and the maximum adsorption value of compatibilizers increased significantly with the increase of the molecular weight of PBMA segment.

From the thermodynamic and kinetic studies, it could be seen that the adsorption of compatibilizers on the QDs surface can be effectively improved when PBMA segment molecular weight increased.

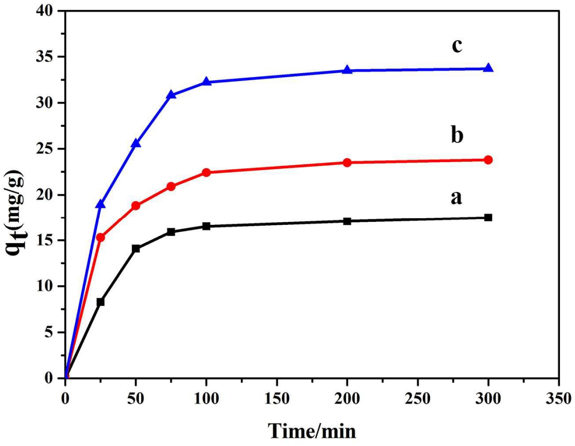

Fig. 2 Effect of the contact time on the adsorption process.

3.2.2 The influences of coating structure of compatibilizers with different PBMA segment molecular weights on optical properties of QDs

UV−visible spectra of QDs that adsorbed different molecular weight compatibilizers showed that QDs had absorption over a wide wavelength range (Fig. 3A). For CdS coated CdSe QDs, the first absorption peak at 450 nm was not evident. This phenomenon had been reported by L.J. An.[25] Fluorescence emission peaks of QDs coated by compatibilizers blue shifted compared with that of original QDs, suggesting the dispersion of QDs was improved after functionalization.[26] In addition, the emission peaks red shifted with the PBMA segment molecular weight of compatibilizers increased. This was because sizes of functionalized QDs increased with the molecular weight of compatibilizers increased. Increasing QDs sizes resulted in red shifts of the luminescence peak due to a reduction in quantum confinement.[27] When QDs adsorbed the compatibilizer with PBMA segment molecular weight 1700, the fluorescence intensity somewhat decreased. This was due to the molecular weight of PBMA was too large, wrapping a plurality of QDs that led to the reunion (Fig. 3B). All the QDs that adsorbed different molecular weight compatibilizers had a wide range of excitation in 350-550nm (Fig. 3C). As shown in Fig. 3D, QDs that adsorbed compatibilizer with PBMA segment molecular weight 850 achieved the highest fluorescence quantum yield.

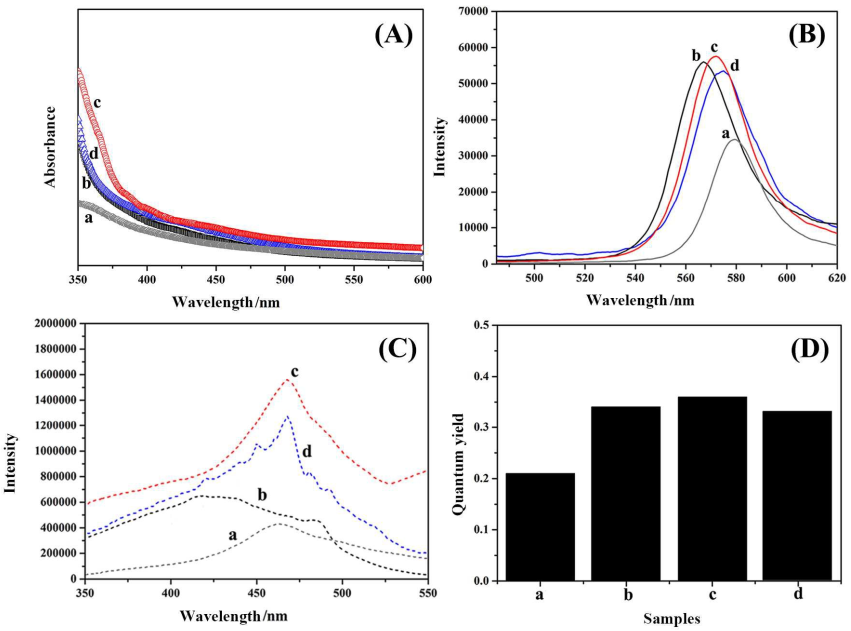

Fig. 3 UV−visible (A), emission (B), excitation (C) spectra and fluorescence quantum yield (D) of QDs that adsorbed different molecular weight compatibilizers (a, original QDs, b, c, d were QDs that adsorbed compatibilizers with PBMA segment molecular weight 420, 850, 1700, and PGMA segment molecular weight 850, respectively.)

3.2.3 The influences of PGMA segment molecular weight on thermodynamics and dynamics of the compatibilization process of QDs in epoxy resin

Based on the above analysis results, the influence of PGMA chain segment molecular weight was further studied, with the PBMA segments molecular weight selected as 850. Titration method was used to investigate influences of PGMA chain segment molecular weight on the degree of QDs surface epoxidation. As shown in Fig. 4, the epoxy value of QDs after coated gradually increased with the contact time, and later flattened after reaching a certain value. Besides, the epoxy value of QDs that adsorbed the compatibilizer with PGMA segments molecular weight 1700 was the highest, which up to 0.395.

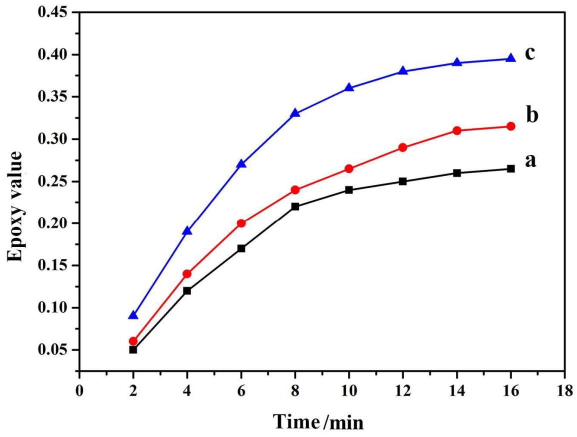

Fig. 4 Epoxy value of QDs that adsorbed different molecular weight compatibilizers for various contact time (a, b, c were QDs that adsorbed compatibilizers with PGMA segment molecular weight 420, 850, 1700, and PBMA segment molecular weight 850, respectively.)

Microcalorimetry was used to measure the enthalpies of dissolution for QDs that adsorbed compatibilizers with different PGMA segment molecular weights dispersing in epoxy resin (Fig. 5). QDs that adsorbed compatibilizer with PGMA segment molecular weight 420 and PBMA segment molecular weight 850 mixed with epoxy resin in t_1=0.86 h, and the curve showed a sharp rise. The exotherm reached the maximum value until t_2=1.02 h, then the curve decreased slowly, and back to baseline in t_3=1.48 h. QDs that adsorbed compatibilizers with PGMA segment molecular weight 850, 1700, and PBMA segment molecular weight 850 mixed with epoxy resin in t_4=2.64 h and t_5=5.05 h, respectively. The trend of microcalorimetric curve b and c were roughly the same as cure a. The enthalpy of dissolution that $\Delta H_a < \Delta H_b < \Delta H_c$ was obtained through curve integral, indicating QDs that adsorbed the compatibilizer with PGMA segment molecular weight 1700 more easily dispersed in epoxy resin.

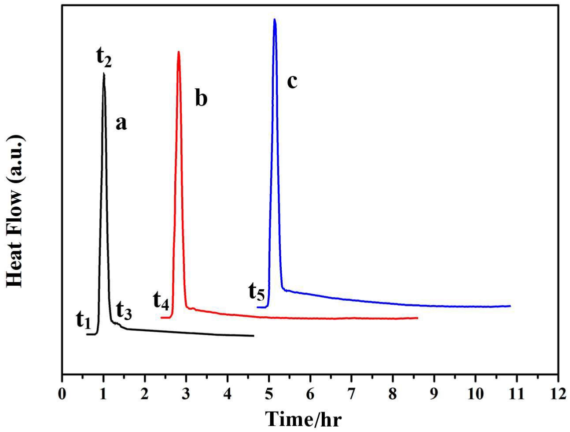

Fig. 5 Microcalorimetric curve for QDs that adsorbed different molecular weight compatibilizers (a, b, c were QDs that adsorbed compatibilizers with PGMA segment molecular weight 420, 850, 1700, and PBMA segment molecular weight 850, respectively.)

Characterization of the particle size of QDs that adsorbed compatibilizers with different PGMA segment molecular weights in epoxy resin was obtained through dynamic light scattering. As shown in Fig. 6, the particle size of QDs clusters decreased over time. Besides, the particle size of QDs clusters that adsorbed compatibilizer with PGMA segment molecular weight 1700 decreased fastest, and already decreased to 13.97 nm after 60 min.

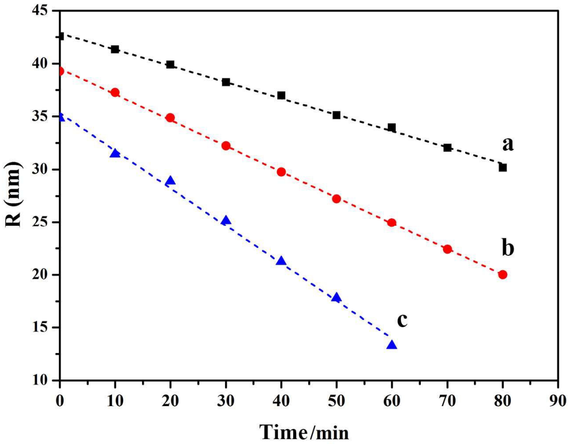

Fig. 6 Particle size of QDs that adsorbed different molecular weight compatibilizers dispersed in epoxy resin (a, b, c were QDs that adsorbed compatibilizers with PGMA segment molecular weight 420, 850, 1700, and PBMA segment molecular weight 850, respectively.)

3.2.4 The influences of coating structure of compatibilizers with different PGMA segment molecular weights on optical properties of QDs

All the QDs that adsorbed different molecular weight compatibilizers had a wide absorption band (Fig. 7A). When the PGMA segment molecular weight of compatibilizer changed from 420 to 850 and then to 1700, the emission peak position of fluorescence emission spectra remained unchanged but the fluorescence emission intensity gradually increased. And the emission peak of functionalized QDs blue shifted compared with the original QDs, indicating that the dispersion of QDs coated with compatibilizers improved (Fig. 7B). The excitation spectra of QDs that adsorbed different molecular weight compatibilizers covered 350-550nm (Fig. 7C). Fluorescence quantum yield of QDs that adsorbed different molecular weight compatibilizers reached a maximum of 43% when the PGMA segment molecular weight was 1700. And there was little effect on the QDs fluorescence quantum yield when the PGMA segment molecular weight further increased (Fig. 7D).

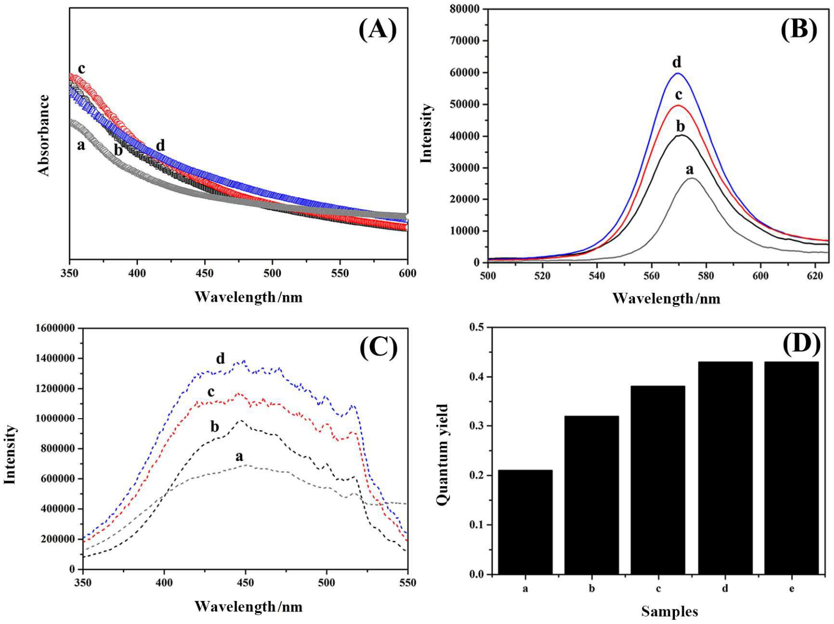

Fig. 7 UV−visible (A), emission (B), excitation (C) spectra and fluorescence quantum yield (D) of QDs that adsorbed different molecular weight compatibilizers (a, original QDs, b, c, d, e were QDs that adsorbed compatibilizers with PGMA segment molecular weight 420, 850, 1700, 2130 and PBMA segment molecular weight 850, respectively.)

The following conclusions could be obtained based on the above study: the increase of PBMA segment molecular weight was beneficial for the compatibilizer to adsorb onto QDs surface. However, when PBMA segment molecular weight was too large, it will cause the single segment covering multiple QDs, reducing the QDs fluorescence yield, and affecting the QDs optical properties. The suitable PBMA segment molecular weight should be controlled in 850. The increase of PGMA segment molecular weight was beneficial for the QDs to disperse in epoxy resin. The fluorescence quantum yield of QDs was also improved with the increase of PGMA segment molecular weight. When the PGMA segment molecular weight was larger than 1700, the change of its molecular weight had little effect on fluorescence yield.

3.3 The properties of QDs/epoxy nanocomposites

CdS coated CdSe QDs functionalized with block copolymer poly(BMA-b-GMA) in which PBMA segment molecular weight 850 and PGMA segment molecular weight 1700 were dispersed in epoxy matrix. Fig. 8 showed confocal laser scanning microscope images of the original and functionalized QDs/epoxy nanocomposites. The nanocomposite containing 0.3 wt% functionalized QDs expressed stronger luminescence and better dispersion of QDs compared to that containing original QDs.

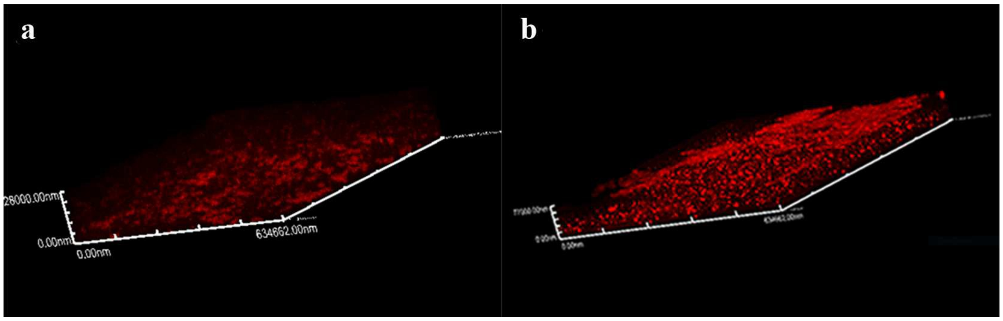

Fig. 8 Three dimensional confocal microscopy images of original QDs/epoxy nanocomposites (a) and functionalized QDs/epoxy nanocomposites (b)

The transparency of the neat epoxy and nanocomposite samples (3 mm thickness) were characterized by their absorption spectra (Fig. 9a). It could be observed that the nanocomposite containing functionalized QDs expressed a transmittance that only had a little decrease compared to neat epoxy. On the contrary, the transmittance of the nanocomposite containing original QDs was obviously much lower than that of the nanocomposite containing the same amount (0.3 wt%) of functionalized QDs. Fluorescent spectra of nanocomposites containing green and red functionalized QDs (weight ratio 1:1) showed a peak at 540nm and a peak at 610nm. Besides, the functionalized QDs/epoxy nanocomposite achieved almost four times the emission intensity than that of original QDs/epoxy nanocomposite (excited light of the emission spectrum was 465 nm) (Fig. 9b).

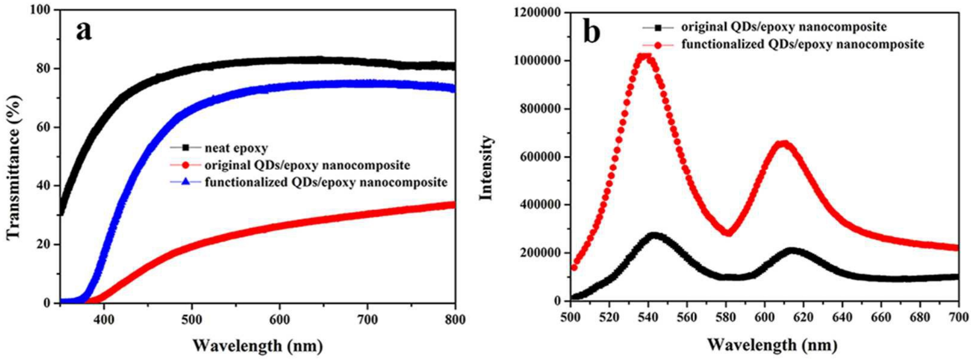

Fig. 9 The transmittance (a) and fluorescent spectra (b) of original and functionalized QDs/epoxy nanocomposites

3.4 Preparation of a white LED encapsulated by dual QDs/epoxy nanocomposite

A white LED was fabricated by coating dual QDs/epoxy nanocomposite (~3mm) onto a 465nm blue InGaN chip. As shown in Fig. 11, the bare chip emitted blue light centered at 465nm. And the LED encapsulated by dual QDs/epoxy nanocomposite showed one blue band (InGaN chip emission), one green band (540 nm QDs emission) and one red band (610nm QDs emission). With the ratio of red QDs increased, the emission around 540nm decreased and the emission around 610nm gradually increased, respectively. When the ratio of green QDs to red QDs was 1:1, the as-prepared white LED showed good performance with CRI, CCT and color coordinates were 69, 6824K and (x=0.3125, y=0.2972), respectively.

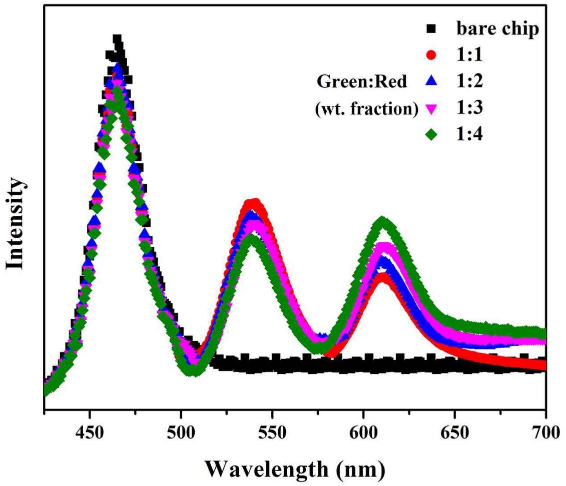

Fig. 10 Photoluminescence spectra of the blue LED encapsulated with nanocomposites containing dual QDs

4. Conclusion

Poly(n-butyl methacrylate)-(glycidyl methacrylate) block copolymer denoted as poly(BMA-b-GMA) had been synthesized by atom transfer radical polymerization (ATRP). Through introducing poly(BMA-b-GMA) as compatibilizer at the interface, transparent and luminescent quantum dots (QDs)/epoxy nanocomposite had been obtained because of improved compatibility. The as-prepared nanocomposite containing 540nm and 610nm light emitting CdS coated CdSe QDs was used to encapsulate blue light emitting (465nm) InGaN LED chip. As a result, a white light dual QDs-LED showed good performance with a color coordinates of (0.3125, 0.2972), CRI of 69 and CCT of 6824K.

Acknowledgements

This work was financially supported by National Natural Science Foundation of China (No. 51203007) and Beijing Natural Science Foundation (No. 2122046).

References

[1] Y.-K. Kim, K.-C. Choi, Y.-K. Baek and P.-W. Shin, Mater. Lett., 2014, 124, 129-132.

[2] E. Fanizza, C. Urso, V. Pinto, A. Cardone, R. Ragni, N. Depalo, M.L. Curri, A. Agostiano, G.M. Farinola and M. Striccoli, J. Mater. Chem., 2014, 2, 5286-5291.

[3] Y. Yang, Y.-Q. Li, S.-Y. Fu and H.-M. Xiao, J. Phys. Chem. C, 2008, 112, 10553-10558.

[4] M. A. Schreuder, J. D. Gosnell, N. J. Smith, M. R. Warnement, S. M. Weiss and S. J. Rosenthal, J. Mater. Chem., 2008, 18, 970-975.

[5] Y.-Q. Li, Y. Yang, C. Q. Sun and S.-Y. Fu, J. Phys. Chem. C, 2008, 112, 17397-17401.

[6] S. Mohan, O. S. Oluwafemi, S. P. Songca, O. A. Osibote, S. C. George, N. Kalarikkal and S. Thomas, New J. Chem., 2014, 38, 155-162.

[7] D. Sun, H.-J. Sue and N. Miyatake, J. Phys. Chem. C 2008, 112, 16002-16010.

[8] M. Agrawal, S. Gupta, N. E. Zafeiropoulos, U. Oertel, R. Häßler and M. Stamm, Macromol. Chem. Phys., 2010, 211, 1925-1932.

[9] Y. Li, J. Tang, L. Huang, Y. Wang, J. Liu, X. Ge, S. C. Tjong, R. K. Y. Li and L. A. Belfiore, Composites Part A, 2015, 68, 1-9.

[10] X. Gong, L. Pan, C. Y. Tang, L. Chen, Z. Hao, W.-C. Law, X. Wang, C. P. Tsui and C. Wu, Composites Part B, 2014, 66, 494-499.

[11] Z.-S. Guo, L. Zhao, J. Pei, Z.-L. Zhou, G. Gibson, J. Brug, S. Lam and S. S. Mao, Macromolecules, 2010, 43, 1860-1866.

[12] R. Y. Hong, J. H. Li, L. L. Chen, D. Q. Liu, H. Z. Li, Y. Zheng and J. Ding, Powder Technol., 2009, 189, 426-432.

[13] R. Y. Hong, L. L. Chen, J. H. Li, H. Z. Li, Y. Zheng and J. Ding, Polym. Adv. Technol., 2007, 18, 901-909.

[14] H.Q. Shi, W.N. Li, L.W. Sun, Y. Liu, H.M. Xiao and S.Y. Fu, Chem. Commun., 2011, 47, 11921-11923.

[15] P.T. Chung, C.T. Yang, S.H. Wang, C.W. Chen, A.S.T. Chiang and C.-Y. Liu, Mater. Chem. Phys., 2012, 136, 868-876.

[16] V. Khrenov, M. Klapper, M. Koch and K. Müllen, Macromol. Chem. Phys., 2005, 206, 95-101.

[17] S. Chen, J. Zhu, Y. Shen, C. Hu and L. Chen, Langmuir 2007, 23, 850-854.

[18] J. J. Huang, Y. B. Ye, Z. Q. Lei, X. J. Ye, M. Z. Rong and M.Q. Zhang, PCCP, 2014, 16, 5480-5484.

[19] W. Zou, Z.-j. Du, H.-q. Li and C. Zhang, Polymer, 2011, 52, 1938-1943.

[20] W. Zou, Z.-j. Du, H.-q. Li and C. Zhang, J. Mater. Chem., 2011, 21, 13276-282.

[21] L. Chen, C. Zhang, Z. Du, H. Li and W. Zou, Mater. Lett., 2013, 110, 208-211.

[22] S. Nizamoglu, T. Ozel, E. Sari and H.V. Demir, Nanotechnology, 2007, 18, 65709 (1-5).

[23] R. Wang, J. Zhang , X. Xu, Y. Wang, L. Zhou, B. Li, Mater. Lett., 2012, 84, 24-26.

[24] J. Wei, C. Zhang, Z. Du, H. Li and W. Zou, J. Mater. Chem. C, 2014, 2, 4177-4185.

[25] D.C. Pan, Q. Wang, J.B. Pang, S.C. Jiang, X.L. Ji and L.J. An, Chem. Mater., 2006, 18, 4253- 4258.

[26] G.R. Bardajee, Z. Hooshyar and F. Mizani, Mater. Sci. Semicond. Process., 2014, 19, 89-94.

[27] N. D. Bronstein, L.F. Li, L. Xu, Y. Yao, V. E. Ferry, A. P. Alivisatos, and R. G. Nuzzo, ACS Nano 2014, 8, 44-53.